Известия вузов России. Радиоэлектроника. 2025. Т. 28, № 3. С. 106–115
Journal of the Russian Universities. Radioelectronics. 2025, vol. 28, no. 3, pp. 106–115

Radar and Navigation

UDC 621.396.62 Original article

https://doi.org/10.32603/1993-8985-2025-28-3-106-115

Autocorrelation Method for Phased Antenna Array Calibration Based on Far-Field Measurement System

Xuan Luong Nguyen[1], Nguyen Trong Nhan[2]✉, Tran Van Thanh[2], Phung Bao Nguyen[3]

[1]VNU University of Science, Hanoi, Vietnam

[2]Air Defense-Air Force Technical Institute, Hanoi, Vietnam

[3]Le Quy Don Technical University, Hanoi, Vietnam

✉ 10th20th30th@gmail.com

Abstract

Introduction. An autocorrelation method can be used for calibration of phased antenna arrays (PAA) in the presence of interference. In scenarios where the PAA size is substantial, the initial elements of post-calibration are designated as a reference element for subsequent comparison with the following antenna elements. However, this method becomes time-consuming when the PAA size increases, also affecting the adaptive calibration proposed in this work. In practical applications, the calibration of PAA may be affected by various factors, such as intentional interference, passive interference, weather conditions, equipment aging, etc. Therefore, the impact of different interference levels on the calibration accuracy of PAA should be investigated. In addition, using a calibration antenna instead of a reference antenna may decrease the calibration accuracy of the received signal.

Aim. To design and investigate a method for calibrating a PAA with high accuracy and low complexity based on an autocorrelation algorithm.

Materials and methods. The efficiency of the developed algorithm was estimated using MATLAB/Simulink-based simulation and experimental validation.

Results. To verify the feasibility of the proposed method for a large-scale antenna array, a 2 × 8 phased array antenna is implemented at 3 GHz. The proposed autocorrelation method for PAA exhibited superior performance over the conventional autocorrelation method. In comparison with the conventional autocorrelation technique, the developed method enhances the peak value of the combined beam in the E-plane by 3.2 and 3.7 dB, respectively. Furthermore, the beams at a distance between two antennas equal 0.625λ were tilted by 1.5 and 8° for the proposed and conventional autocorrelation methods, respectively.

Conclusion. The validation through actual measurement data confirmed that the proposed autocorrelation method is more accurate than conventional methods in determining amplitude and phase offsets. The paper points out that the proposed autocorrelation calibration method performs well in large-scale on-site and factory-level calibration, being also effective in scenarios under the presence of external interference.

Keywords: phased array antenna, PAA, correlation function, far-field measurement system, scanning time, interference source

For citation: Xuan Luong Nguyen, Nguyen Trong Nhan, Tran Van Thanh, Phung Bao Nguyen. Autocorrelation Method for Phased Antenna Array Calibration Based on Far-Field Measurement System. Journal of the Russian Universities. Radioelectronics. 2025, vol. 28, no. 3, pp. 106–115.
doi: 10.32603/1993-8985-2025-28-3-106-115

Conflict of interest. The authors declare no conflicts of interest.

Submitted 28.04.2025; accepted 06.06.2025; published online 30.06.2025

Introduction. In contemporary radio and communication systems, phased antenna arrays (PAA) find wide application [1–3]. PAAs facilitate control over the shape of the radiation pattern and the position of the main lobe, referred to as a beam, of the respective antenna system. Each PAA channel includes ultra-high frequency components to monitor the amplitude and phase of the passing signal. These components are characterized by amplitude and phase errors which adversely affect the shape of the radiation pattern and its characteristics [4–6]. In addition, mismatches in the amplitude and phase characteristics can be caused by external factors. In this context, mention should be made of various natural physical noises and disturbances generated by external influences [7–9]. Therefore, in order to compensate for these errors, the PAA must be calibrated not only at the manufacturing stage, but also during operation [10–12].

A significant objective of the PAA calibration process is to minimize the time required for calibration and to mitigate the impact of environmental factors on the resulting radiation pattern, whether in factory settings or at open measurement sites [13–17]. Development of efficient measures to deal with the aforementioned issue require utilization of far-field calibration techniques based on differences, namely the rotating-element electric-field vector (REV) [18–24] and autocorrelation methods [25]. The research presented in [25] demonstrated that the autocorrelation approach exhibited superior precision in the calibration of amplitude and phase, in comparison with REV methods. In cases where the number of antenna elements exceeds two, the autocorrelation method is continued to the last element. In scenarios where the PAA size is substantial, the initial elements are designated as a reference element for subsequent comparison with the following antenna elements.

However, the time required for this method [25] increases significantly under an increase in the array antenna size, thus affecting the adaptive calibration proposed in this work. In practical applications, the calibration of PAAs may be affected by various factors, such as intentional interference, passive interference, weather conditions, equipment aging, etc. Therefore, it is necessary to investigate the effects of different levels of interference on the calibration accuracy of PAA. In addition, using a calibration antenna instead of a reference antenna may lead to a decrease in the accuracy of the received signal calibration.

In this regard, this paper aims to design and investigate a method for calibrating a phased antenna array with high accuracy and low complexity based on an autocorrelation algorithm. The paper is structured as follows: section 1 introduces the theory of the proposed autocorrelation method, section 2 details the experimental setup of the developed algorithm, and section 3 offers concluding remarks.

Description of the Developed Algorithm. Fig. 1 illustrates the PAA calibration method based on the autocorrelation algorithm. The method is composed of the following components: The linear PAA with N antenna elements has a total length $D=(N-1)d$, where d – distance between two calibration receive antennas; multipliers; a block for determining w_i; a block for calculating a_i, and an adder.

The subsequent section provides a detailed exposition of the mathematical model of the PAA calibration process in the context of the specified case study:

a) the reception of signals is to be conducted through channels:

$$x_i(t)=s_i(t)+n_i(t),$$

where $s_i(t)=A_i(t)e^{j\beta_i(t)}$ – the complex useful signal received at the *i*-th channel, i = 1, 2, ..., N $\left(A_i(t)\right.$ – the amplitude of the $s_i(t)$; $\beta_i(t)$ – the phase of the $\left.s_i(t)\right)$; $n_i(t)$ – internal and external noises;

b) multiply $x_i(t)$ with $x_0(t)$. The signal $X_i(t)$ is thus expressed as follows:

$$X_i(t)=x_i(t)x_i(t)=\left(s_i(t)+n_i(t)\right)\left(s_0(t)+n_0(t)\right)=$$
$$=s_i(t)s_0(t)+s_i(t)n_0(t)+n_i(t)s_0(t)+n_i(t)n_0(t),$$

where $x_0(t)=s_0(t)+n_0(t)$ – the complex reference signal; $s_0(t)=A_0(t)e^{j\beta_0(t)}$ $\left(A_0(t)\right.$ – the amplitude of the $x_0(t)$; $\beta_0(t)$ – the phase of the $\left.x_0(t)\right)$; $n_0(t)$ – the internal noise at the reference channel;

c) determine the maximum value of the autocorrelation function $X_i(t)$ in the block for finding the values w_i:

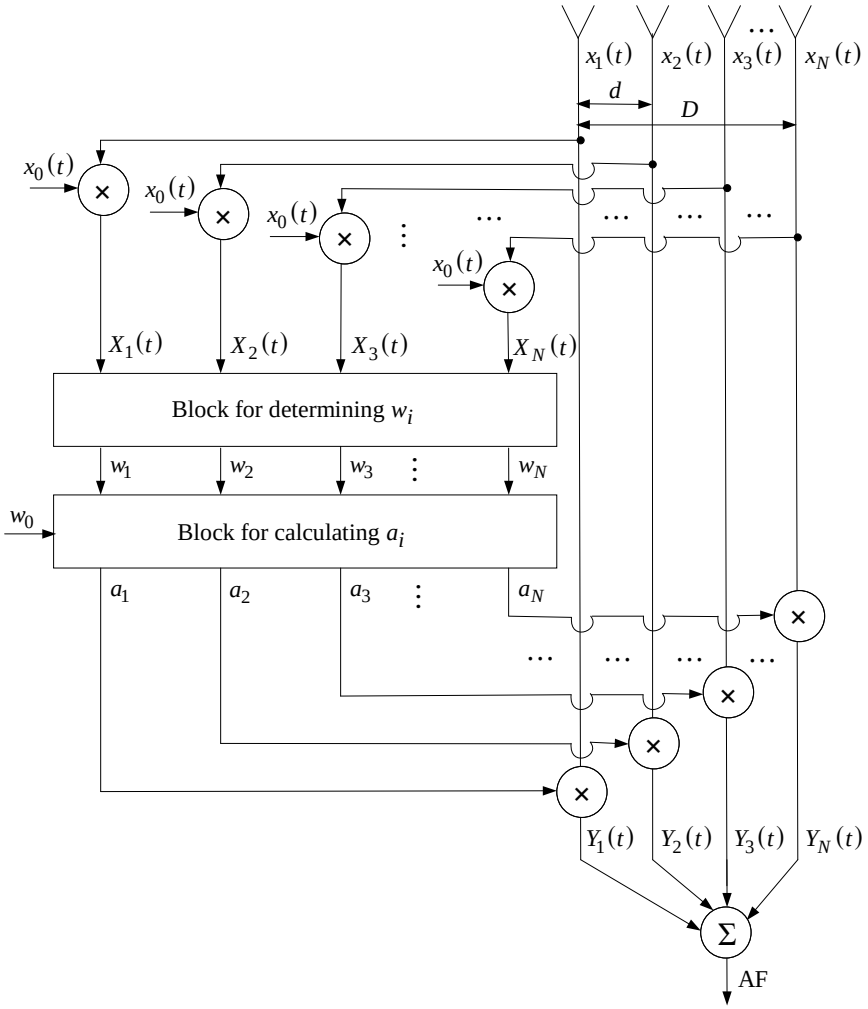

Fig. 1. Ray diagram for PAA calibration method based on autocorrelation algorithm

$$w_i = \max\left(X_i(t)\right) = \max\left(x_i(t)x_0(t)\right) =$$
$$= \max\left(s_i(t)s_0(t) + s_i(t)n_0(t) + n_i(t)s_0(t) + n_i(t)n_0(t)\right),$$

where $X_i(t)$ – the autocorrelation function of the complex received signal $x_i(t)$ and the complex reference signal $x_0(t)$;

d) the weight a_i required to compensate for the input signal of the *i*-th channel can be calculated according to the following:

$$a_i = \frac{w_0}{w_i} = \frac{\max\left(X_0(t)\right)}{\max\left(X_i(t)\right)} = \frac{\max\left(x_0(t)x_0(t)\right)}{\max\left(x_i(t)x_0(t)\right)} =$$
$$= \frac{\max\left(s_0(t)s_0(t) + s_0(t)n_0(t) + n_0(t)s_0(t) + n_0(t)n_0(t)\right)}{\max\left(s_i(t)s_0(t) + s_i(t)n_0(t) + n_i(t)s_0(t) + n_i(t)n_0(t)\right)} =$$
$$= \frac{\max\left(s_0^2(t) + 2s_0(t)n_0(t) + n_0^2(t)\right)}{\max\left(s_i(t)s_0(t) + s_i(t)n_0(t) + n_i(t)s_0(t) + n_i(t)n_0(t)\right)};$$

e) multiply the complex received signal $x_i(t)$ with the weight a_i:

$$Y_i(t) = X_i(t)a_i =$$
$$= \left(s_i(t)s_0(t) + s_i(t)n_0(t) + n_i(t)s_0(t) + n_i(t)n_0(t)\right) \times$$
$$\times \frac{\max\left(s_0^2(t) + 2s_0(t)n_0(t) + n_0^2(t)\right)}{\max\left(s_i(t)s_0(t) + s_i(t)n_0(t) + n_i(t)s_0(t) + n_i(t)n_0(t)\right)};$$

f) the expression of the coefficient array at the output of the adder:

$$AF_i = Y_1(t) + Y_2(t) + Y_3(t) + \ldots + Y_N(t) = \sum_{i=1}^{N} Y_i(t) =$$
$$= \sum_{i=1}^{N}\left[\frac{\left(s_i(t)s_0(t) + s_i(t)n_0(t) + n_i(t)s_0(t) + n_i(t)n_0(t)\right)}{\max\left(s_i(t)s_0(t) + s_i(t)n_0(t) + n_i(t)s_0(t) + n_i(t)n_0(t)\right)} \times\right.$$
$$\left.\times \frac{\max\left(s_0^2(t) + 2s_0(t)n_0(t) + n_0^2(t)\right)}{\max\left(s_i(t)s_0(t) + s_i(t)n_0(t) + n_i(t)s_0(t) + n_i(t)n_0(t)\right)}\right].$$

The proposed method for determining the phase and amplitude shifts of signals involves newly introduced steps 3–6, which are of critical importance.

Results and Discussion.

1. Experimental Setup. As demonstrated in Fig. 2, the amplitude and phase errors of the signals are determined using a calibrated system. The implementation of this system is contingent upon the utilization of the proposed method. The catalogue of key components employed in the experiment is presented in Tab. 1. Fig. 3, *a* depicts the signal processing block. Fig. 3, *b* presents the antennas in the 2 × 8 to be calibrated, while Fig. 3, *c* illustrates the reference antennas, including arrangements. The reference antennas in the 1 × 4 are used to determine the maximum value of the autocorrelation function accurately (Fig. 3, *c*). The calibration system of PAA is subject to regulation using a control panel, as illustrated in Fig. 4.

The experimental process (Fig. 5) goes as follows:

Step 1. Antenna *1* (red square), antenna *2* (red square), antenna *9* (red square), and antenna *10* (red square) are calibrated through reference *1* (blue square) using the proposed method as shown in Fig. 4, *b*.

Step 2. Antenna *3* (red square), antenna *4* (red square), antenna *11* (red square), and antenna *12* (red square) are calibrated through reference *2*.

Step 3. Antenna *5* (red square), antenna *6* (red square), antenna *13* (red square), and antenna *14* (red square) are calibrated through reference *3*.

Step 4. Antenna *7* (red square), antenna *8* (red square), antenna *15* (red square), and antenna *16* (red square) are calibrated through reference *4*.

In comparison with the method in [25], the proposed reference array allows the scanning time to

Tab. 1. Components of experimental design

No.	Components	Number of components
1	Laptop with MATLAB 2024a	1
2	Rotary control block	1
3	Rotary platform	1
4	Power supply 12 V, 5 V	2
5	Zynq UltraScale + RFSoC ZCU216 Evaluation Kit	1
6	Interference source	1
7	Antennas to be calibrated	2 × 8
8	Reference antennas	1 × 4

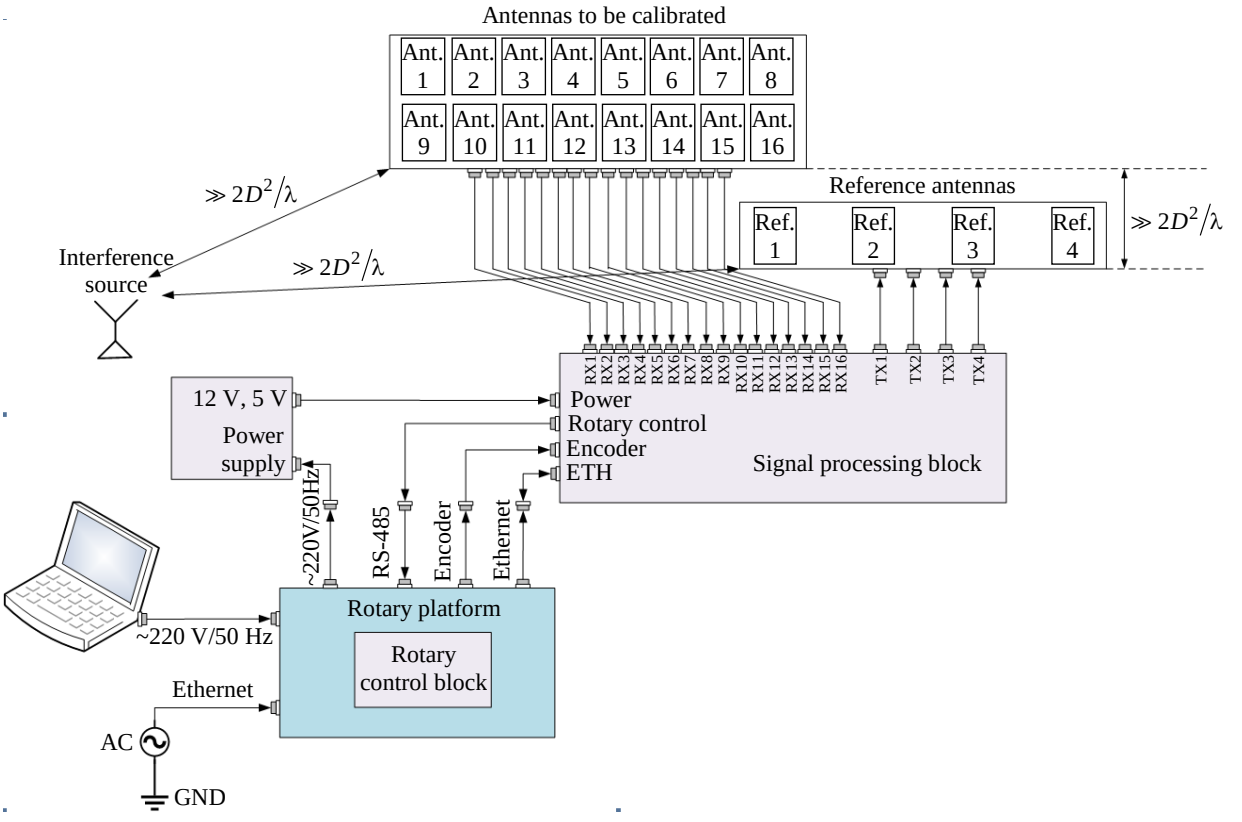

Fig. 2. Schematic calibration diagram for experimental design

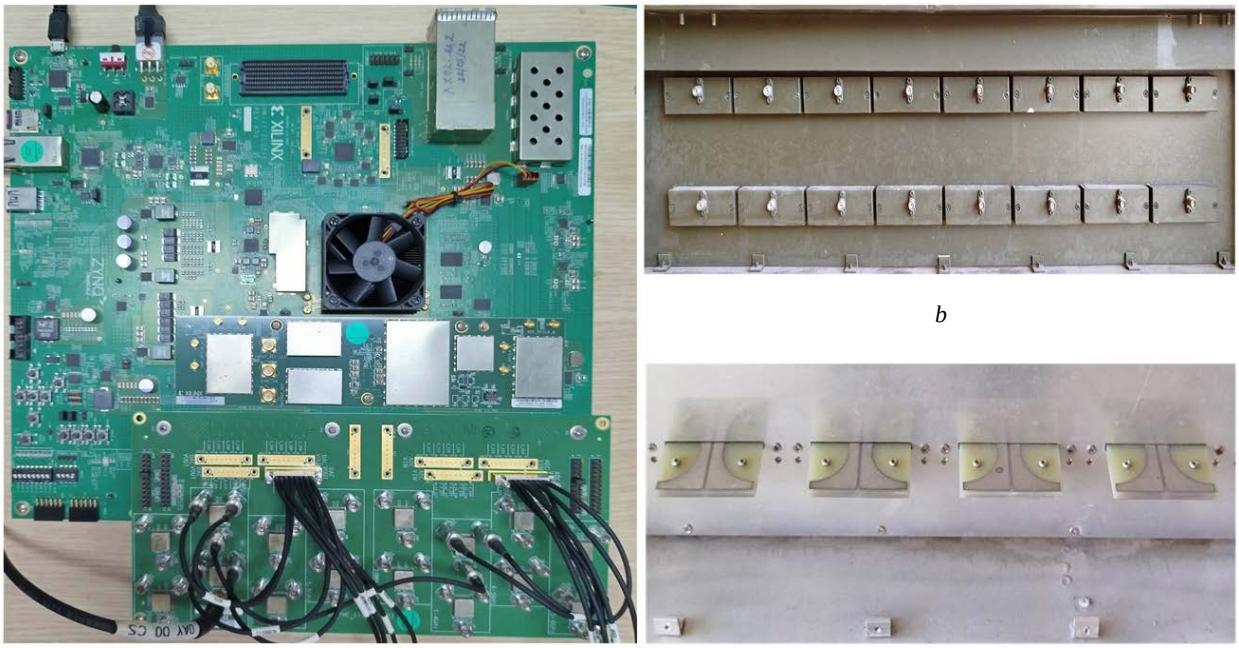

a *b* *c*

Fig. 3. Components of calibration system: *a* – signal processing block; *b* – 2×8 phased array antenna for test; *c* – 1×4 reference (transmitting) antennas

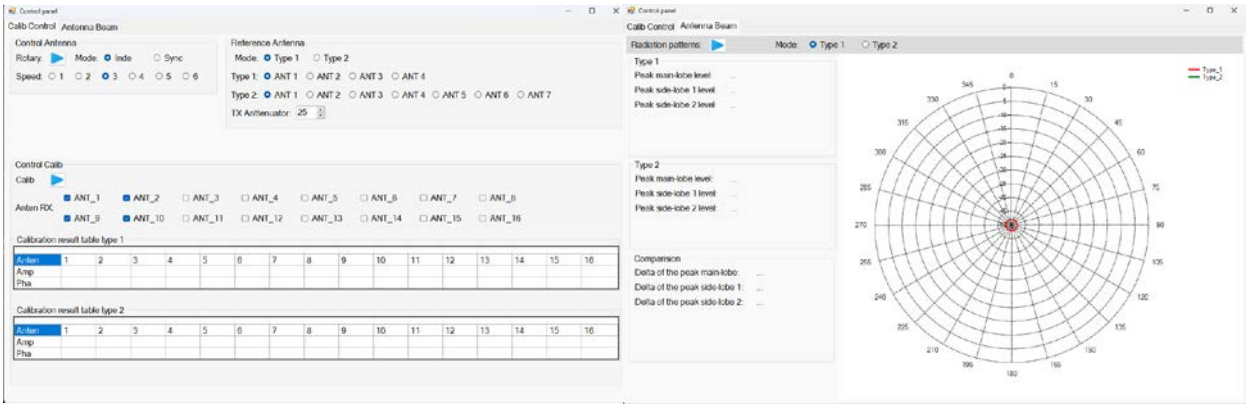

Fig. 4. Control panel of the experiment

be optimized, due to using only four reference elements instead of seven reference elements in [25].

The subsequent research step is aimed at calibrating the system that is utilized to demonstrate the radiation patterns of the array, in the aftermath of the implementation of amplitude and phase perturbations on the received signals, employing the autocorrelation techniques as depicted in Fig. 6. To investigate the efficacy of the developed method using the presented calibration system, 10 tests were carried out. The initial data are shown in Tab. 2.

2. Measurement Campaigns and Comments. The developed method was investigated based on the experimental setup proposed in Section 2.1. The results of amplitude and phase error measurements are shown in Fig. 7. The superior performance of the proposed autocorrelation method in PAA compared to the conventional autocorrelation method is demonstrated. Fig. 7 shows that for different calibration methods, the amplitude and phase errors decrease with an increase in SNR. For example, for the first antenna element, using the proposed method, with the increase of the SNR from 0 to 10 dB, the amplitude error decreases by 0.16, and the phase error decreases by 15.49°. For comparison, when using the conventional method, the amplitude error equals 0.17, and the phase error equals 8.18°.

It is worth noting that in the conventional method, an increase in the PAA size is associated with an increase in the amplitude and phase errors. This is due to the consistent dependence of the

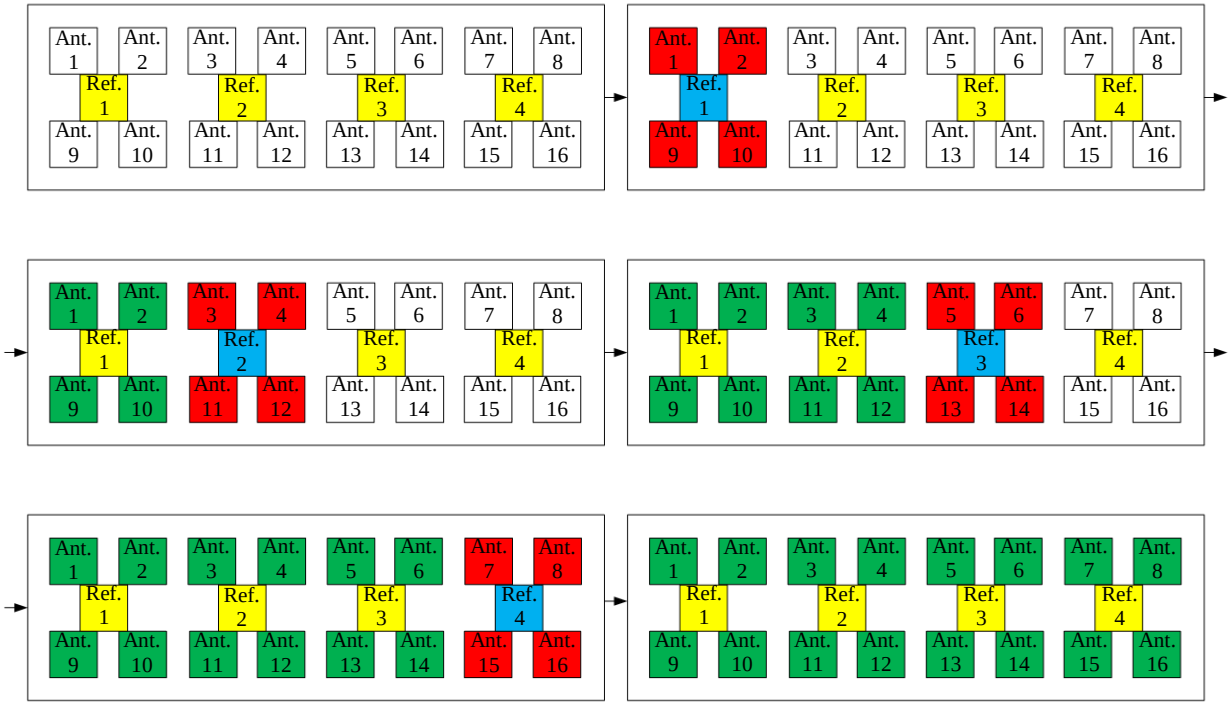

Fig. 5. Calibration sequence with a horizontal scanning direction in x-y plane view: before calibration (white), calibrated (red), after calibration (green), selected reference (blue), unselected reference (yellow) antennas

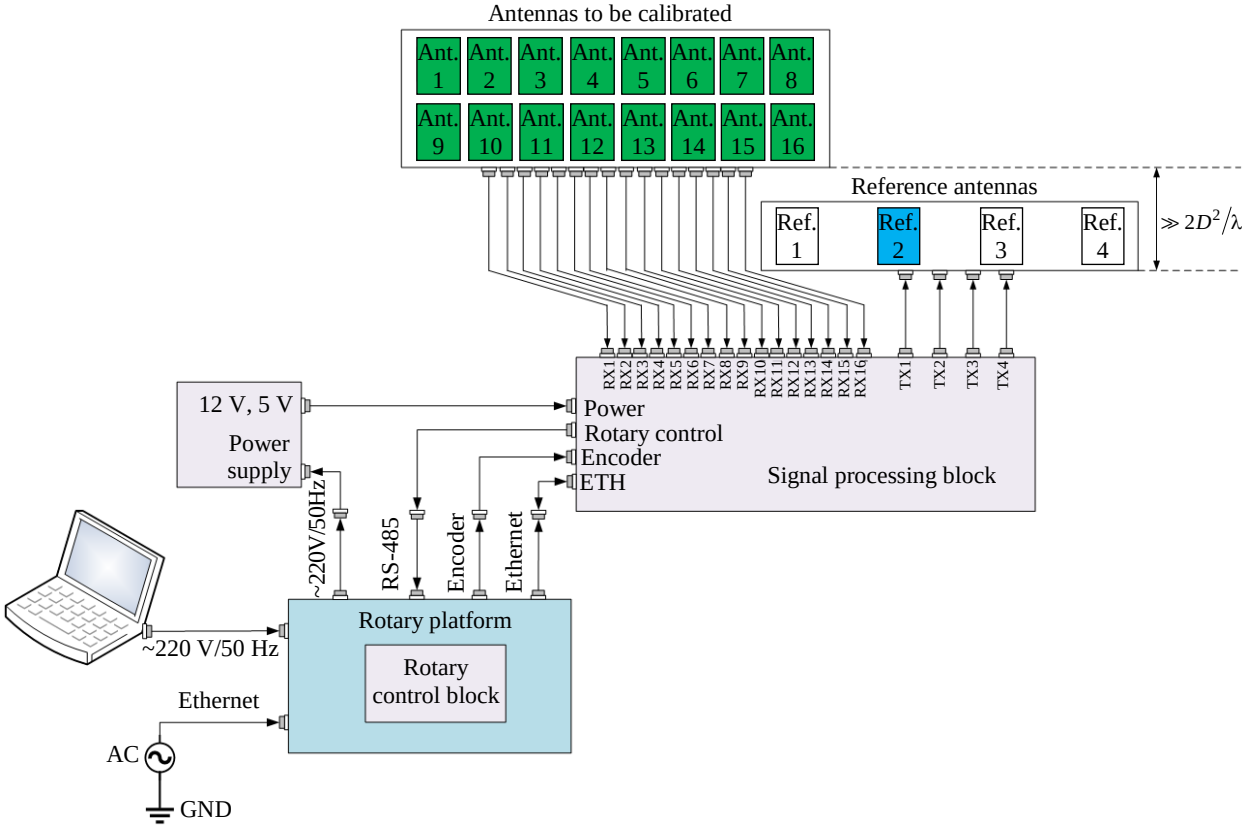

Fig. 6. Calibration diagram for drawing the radiation patterns after calibration using the difference-based autocorrelation methods: the array antennas in the *X*–*Y* plane view

Tab. 2. Initial parameter values

No.	Parameters	Values
1	Frequency of the received signal	3 GHz
2	Distance between two calibration receive antennas	6.25 cm
3	Distance between the calibration antennas and the reference antennas	3 m
4	Distance between the reference antennas and the interference source	2 m
5	Distance between the calibration antennas and the interference source	4 m
6	SNR	0.10 dB

selection of the standard calibration channel. Thus, with the increase of antenna elements from 1 to 16: when SNR at 0 dB amplitude errors increase from 0.32 to 0.42, and phase errors increase from 20.5 to 30°; when SNR at 10 dB amplitude errors – 0.15 to 0.25, and phase errors increase from 5.01 to 9.9°. Meanwhile, for the proposed method, these errors do not vary significantly from their mean value. For example, for the case of SNR at 0 dB, the amplitude errors do not deviate substantially from 0.3, and the phase errors do not significantly differ from 11.9°; for the case of SNR at 10 dB, the amplitude errors – 0.14, and the phase errors do not significantly differ from 2.79°. In addition, at each calibration step, the amplitude and phase of the four antenna elements are almost equal.

As demonstrated in Fig. 8, the employment of difference-based autocorrelation methods yielded specific calibration outcomes. It is evident from this figure that alterations in the azimuth angle of the transceiver antenna, designated as φ_{tr}, do not exert a significant influence on the precision of the calibration process, at least within the context of the present investigation. Fig. 8 shows that, in comparison with the conventional autocorrelation technique, the developed method enhances the peak value of the combined beam in the E-plane by 3.2 and 3.7 dB, respectively. Furthermore, the beams at a distance between two antennas at $d = 0.625\lambda$ were tilted by 1.5, 8° for the proposed and conventional autocorrelation methods, respectively.

Conclusion. This paper sets forth an alternative methodology for the calibration of autocorrelation. The efficacy of this approach is confirmed by its

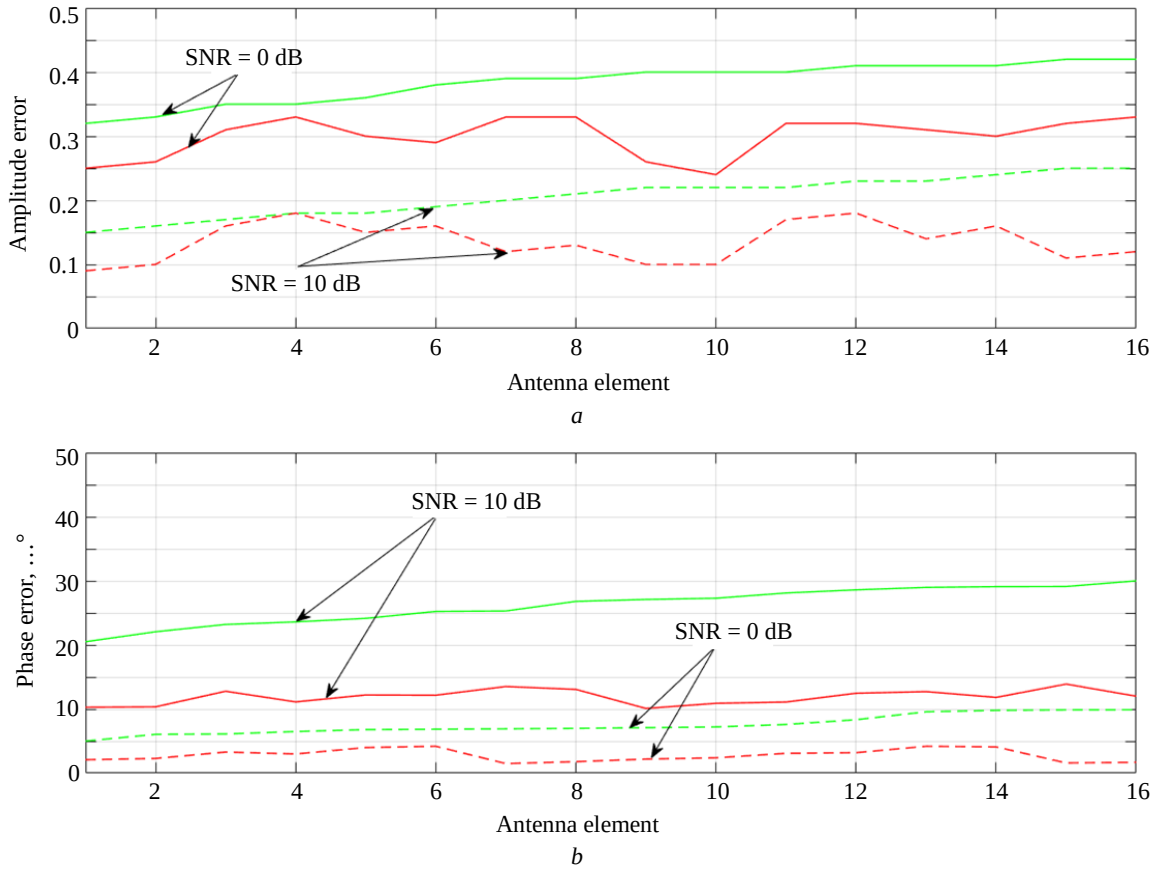

Fig. 7. Dependence of amplitude (*a*) and phase errors (*b*) on the number of antenna elements using different calibration methods; the proposed autocorrelation method (red) and the conventional method (green)

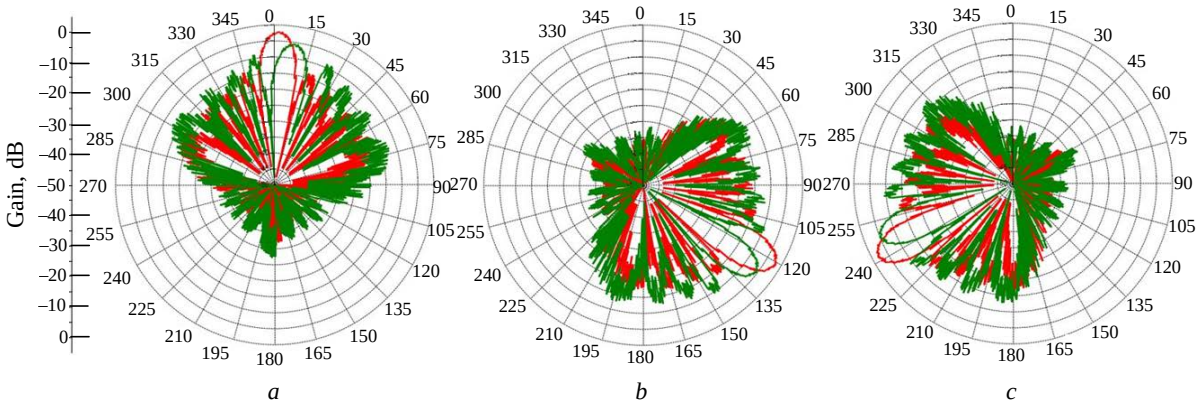

Fig. 8. Radiation pattern of the combined beam after calibration in the *E*-plane: *a* – $\varphi_{tr.}$ = 0°; *b* – $\varphi_{tr.}$ = 120°; *c* – $\varphi_{tr.}$ = 240°; proposed autocorrelation method – red; conventional autocorrelation method – green

capacity to enhance the precision of calibration, while concomitantly effectuating a reduction in errors that may be attributable to amplitude and phase under the conditions of both internal and external noise disturbances. This comprehensive exploration from theory to experiment is of great significance for understanding the application of autocorrelation algorithms in calibration of phased antenna arrays. The proposed autocorrelation calibration method was compared and analyzed with conventional autocorrelation methods. Through actual measurement data, the authors demonstrated that the proposed autocorrelation methods are more accurate than conventional methods in determining amplitude and phase offsets.

The results indicate that the proposed autocorrelation calibration method performs well in large-scale on-site and factory-level calibration, being also effective under the presence of external interference. This finding is of great significance for applying phased antenna arrays in inhomogeneous environments. The data is recorded for use in the automatic calibration sub-system of the PAA during operation. However, this paper has not been focused on analyzing the calibration process in the context of signal reception and processing with non-uniform distribution of antenna elements. Consequently, further research will encompass the study and development of an algorithm for signal calibration in interference conditions for PAA with non-uniform antenna element distribution.

Author's contribution

Xuan Luong Nguyen, computer modeling; processing of experimental results; paper editing, formulating conclusions.

Nguyen Trong Nhan, supervision of scientific work; setting tasks; processing of experimental results; formulating conclusions.

Tran Van Thanh, literature review; processing of experimental results; paper editing.

Phung Bao Nguyen, literature review; processing of experimental results; paper editing.

All authors participated in the discussion of the results and in the preparation of the paper.

References

1. He G., Gao X., Zhang R., Sun L., Zhou H. Phased Array Antenna Basics. Multibeam Phased Array Antennas as Satellite Constellation Ground Station. Modern Antenna. Singapore, Springer, 2024, pp. 9–37. doi: 10.1007/978-981-99-7910-3_2

2. Díaz J. D., Salazar-Cerreno J. L., Ortiz J. A., Aboserwal N. A., Lebrón R. M., Fulton C. A Cross-Stacked Radiating Antenna with Enhanced Scanning Performance for Digital Beamforming Multifunction Phased-Array Radars. IEEE Transactions on Antennas and Propagation. 2018, vol. 66, iss. 10, pp. 5258–5267. doi: 10.1109/TAP.2018.2862252

3. Fenn A. J., Hurst P. T. Phased Array Antenna Theory. Ultrawideband Phased Array Antenna Technology for Sensing and Communications Systems. Cambridge, MIT Press, 2015, pp. 91–133.

4. Sorace R. Phased array calibration. Proc. IEEE Intern. Conf. on Phased Array Systems and Technology (Cat. no. 00TH8510), Dana Point, USA, 21–25 May 2000. IEEE, 2000, pp. 533–536. doi: 10.1109/PAST.2000.859013

5. Tang S., Wang Z., Pan C., Su R., Fan W., Gao S. A Fast and Efficient Calibration Method for Phased Array Antennas Using Fourier-Structured Excitation Matrix. IEEE Transactions on Antennas and Propagation. 2023, vol. 71, no. 3, pp. 2290–2299. doi: 10.1109/TAP.2023.3234814

6. Fulton C., Chappell W. Calibration techniques

for digital phased arrays. IEEE Intern. Conf. on Microwaves, Communications, Antennas and Electronics Systems, Tel Aviv, Israel, 09–11 Nov. 2009. IEEE, 2009, pp. 1–10.
doi: 10.1109/COMCAS.2009.5385979

7. Lier E., Zemlyansky M., Purdy D., Farina D. Phased array calibration and characterization based on orthogonal coding: Theory and experimental validation. IEEE Intern. Symp. on Phased Array Systems and Technology, Waltham, USA, 12–15 Oct. 2010. IEEE, 2010, pp. 271–278.
doi: 10.1109/ARRAY.2010.5613357

8. Xiao Y., Fan Y., Cheng Y. J. Phased Array Antenna With Self-Calibration Network and Improved Scanning Performance. IEEE Antennas and Wireless Propagation Let. 2023, vol. 22, no. 6, pp. 1226–1230.
doi: 10.1109/LAWP.2023.3237211

9. Lee D. -H., Seo J. -W., Lee M. -S., Chung D., Lee D., Bang J. -H., Satriyotomo B., Pyo S. An S-Band-Receiving Phased-Array Antenna with a Phase-Deviation-Minimized Calibration Method for LEO Satellite Ground Station Applications. Electronics. 2022, vol. 11, iss. 23, art. no. 3847.
doi: 10.3390/electronics11233847

10. Liu H., Guan T., Fu C., Zhang S., Xu X., Xu Z., Qing A., Lin X. Improving Scanning Performance of Patch Phased Array Antenna by Using a Modified SIW Cavity and Sequential Rotation Technique. Electronics. 2024, vol. 13, iss. 9, art. no. 1776.
doi: 10.3390/electronics13091776

11. Li R., Zhang J., Li C., Li Y., Tian B., Wu C. An Accurate Mid-Field Calibration Technique for Large Phased Array Antenna. 6th Asia-Pacific Conf. on Antennas and Propagation (APCAP), Xi'an, China, 16–19 Oct. 2017. IEEE, 2017, pp. 1–3.
doi: 10.1109/APCAP.2017.8420685

12. Zhou R., Hu Z., Zhao Q., Chen G., Tao J. Absolute Field Calibration of Receiver Antenna Phase Center Models for GPS/BDS-3 Signals. J. Geodesy. 2023, vol. 97, art. no. 83.
doi: 10.1007/s00190-023-01773-7

13. Pöhlmann R., Zhang S., Staudinger E., Dammann A., Hoeher P. A. Simultaneous Localization and Antenna Calibration. 16th Europ. Conf. on Antennas and Propagation (EuCAP), Madrid, Spain, 27 March–01 Apr. 2022. IEEE, 2022, pp. 1–5.
doi: 10.23919/EuCAP53622.2022.9769393

14. Horváth K. A., Ill G., Milánkovich Á. Calibration Method of Antenna Delays for UWB-Based Localization Systems. IEEE 17th Intern. Conf. on Ubiquitous Wireless Broadband (ICUWB), Salamanca, Spain, 12–15 Sept. 2017. IEEE, 2017, pp. 1–5.
doi: 10.1109/ICUWB.2017.8250969

15. Lee Y.-S., Yoon T., Kim M., Lee S., Jung B., Oh J. A Design and Characterization Method of a Scalable Large Transmitting Array for Wireless Power Transfer. IEEE Transactions on Microwave Theory and Techniques, 2024, pp. 1–13.
doi: 10.1109/TMTT.2024.3487911

16. Linder M., Meinecke B., Halici E., Schwarz D., Waldschmidt C. Highly Efficient Calibration of Antenna Arrays by Active Targets in the Near-Field. IEEE Open J. of Antennas and Propagation. 2023, vol. 4, pp. 326–338.
doi: 10.1109/OJAP.2023.3253942

17. Jones D. L., Bagri D. S., Miyatake H. C., Tehrani B. J., Gatti M. S., Cooper H. W. Calibration of Antennas During Construction or Expansion of Radio Arrays. IEEE Aerospace Conf., Big Sky, USA, 01–08 March 2008. IEEE, 2008, pp. 1–8.
doi: 10.1109/AERO.2008.4526308

18. Wang B., Yan Li, Tian B. Rotating-Element Electric-Field Vector (REV) Calibration Method Based on Power Measurement for Phased Array Antenna. Intern. Applied Computational Electromagnetics Society Symp. (ACES), Suzhou, China, 01–04 Aug. 2017. IEEE, 2017, pp. 1–2.

19. Zhang Y., Gao, Liu J. Single Reference Element Rotating-Element Electric-Field Vector Method for Phased Array Antenna Calibration. Systems Engineering and Electronics. 2024, vol. 46, iss. 5, pp. 1525–1534.

20. Yoon H.-J., Min B.-W. Improved Rotating-Element Electric-Field Vector Method for Fast Far-Field Phased Array Calibration. IEEE Transactions on Antennas and Propagation. 2021, vol. 69, no. 11, pp. 8021–8026.
doi: 10.1109/TAP.2021.3083796

21. Liu M., Feng Z. Combined Rotating-element Electric-field Vector (CREV) Method for nearfield Calibration of Phased Array Antenna. Intern. Conf. on Microwave and Millimeter Wave Technology, Guilin, China, 18–21 Apr. 2007. IEEE, 2007, pp. 1–4.
doi: 10.1109/ICMMT.2007.381281

22. Su Y., Song Z., Zhang S., Gong S. Determination of Excitation Amplitude and Phase for Wide-Band Phased Array Antenna Based on Spherical Wave Expansion and Mode Filtering. Electronics. 2022, vol. 11, iss. 21, art. no. 3479.
doi: 10.3390/electronics11213479

23. Wang J. P., Tsai Y.-L., Chen W.-J., Chen J.-H., Hwang R.-B. A Fast Phased Array System Calibration Method by Fully Utilising In-Built Beamformers. IEEE Conf. on Antenna Measurements and Applications (CAMA), Guangzhou, China, 14–17 Dec. 2022. IEEE, 2022, pp. 1–2.
doi: 10.1109/CAMA56352.2022.10002539

24. Pan C., Ba X., Tang Y., Zhang F., Zhang Y., Wang Z., Fan W. Phased Array Antenna Calibration Method Experimental Validation and Comparison. Electronics. 2023, vol. 12, iss. 3, art. no. 489.
doi: 10.3390/electronics12030489

25. Nguyen X. L., Nhan N. T., Dang Thi T. T., Thanh T. V., Nguyen P. B., Trien N. D. Phased Array Antenna Calibration Based on Autocorrelation Algorithm. Sensors. 2024, vol. 24, iss. 23, art. no. 7496.
doi: 10.3390/s24237496

Information about the authors

Xuan Luong Nguyen, Systems Engineer of the Research Institute of Radio Navigation Systems, Researcher of Air Defense – Air Force Technical Institute, Vietnam. PhD student of the Department of Radio Physics of VNU University of Science (Vietnam). The author of 3 scientific publications. Area of expertise: ultra-high frequency radio engineering; systems engineering of multifunctional systems.
Address: VNU University of Science, 334, Nguyen Trai, Hanoi 100000, Vietnam
E-mail: huunghiht@gmail.com
https://orcid.org/0000-0002-9222-2502

Nguyen Trong Nhan, Cand. Sci. (Eng.) (2023), Researcher of Air Defense – Air Force Technical Institute (Vietnam). The author of more than 30 scientific publications. Area of expertise: radio engineering and telecommunications.
Address: Air Defense-Air Force Technical Institute, 166, Hoang Van Thai, Hanoi 11400, Vietnam
E-mail: 10th20th30th@gmail.com
https://orcid.org/0000-0001-6626-893X

Tran Van Thanh, Researcher of Air Defense – Air Force Technical Institute (Vietnam). The author of 2 scientific publications. Area of expertise: radio engineering and telecommunications.
Address: Air Defense-Air Force Technical Institute, 166, Hoang Van Thai, Hanoi 11400, Vietnam.
E-mail: tranthanhtat@gmail.com
https://orcid.org/0009-0000-5213-7349

Phung Bao Nguyen, Cand. Sci. (Eng.) (1996), Lecturer of the Department of Electronic Technology of Institute of System Integration of Le Quy Don Technical University. The author of 30 scientific publications. Area of expertise: radar information processing; radio-electronic and radar technology; systems engineering.
Address: Le Quy Don Technical University, 236, Hoang Quoc Viet, Hanoi 11917, Vietnam
E-mail: nguyenphungbao@lqdtu.edu.vn